

The Surprising Crab Nebula

E. Striani, M. Tavani, V. Vittorini
 INAF/IASF-Roma, I-00133 Roma, Italy

We will present our study of the flux and spectral variability of the Crab above 100 MeV on different timescales ranging from days to weeks. In addition to the four main intense and day-long flares detected by AGILE and Fermi-LAT between Sept. 2007 and Sept. 2012, we find evidence for week-long and less intense episodes of enhanced gamma-ray emission that we call “waves”. Statistically significant “waves” show timescales of 1-2 weeks, and can occur by themselves or in association with shorter flares. The Sept. - Oct. 2007 gamma-ray enhancement episode detected by AGILE shows both “wave” and flaring behavior. We extend our analysis to the publicly available Fermi-LAT dataset and show that several additional “wave” episodes can be identified. We discuss the spectral properties of the September 2007 “wave”/flare event and show that the physical properties of the “waves” are intermediate between steady and flaring states. Plasma instabilities inducing “waves” appear to involve spatial distances $l \sim 10^{16}$ cm and enhanced magnetic fields $B \sim (0.5-1)$ mG. Day-long flares are characterized by smaller distances and larger local magnetic fields. Typically, the deduced total energy associated with the “wave” phenomenon ($E_w \sim 10^{42}$ erg, where E_w is the kinetic energy of the emitting particles) is comparable with that associated to the flares, and can reach a few percent of the total available pulsar spindown energy. Most likely, flares and waves are the product of the same class of plasma instabilities that we show acting on different timescales and radiation intensities.

1. Introduction

The Crab Nebula (the remnant of a Supernova explosion witnessed by Chinese astronomers in 1054) is powered by a very powerful pulsar (of period $P = 0.33$ ms, and spindown luminosity $L_{sd} \simeq 5 \times 10^{38}$ erg s⁻¹) (see e.g., Hester [2008]). The pulsar is energizing the whole system through the interaction of the particle and wave output within the surrounding Nebula (of average magnetic field $\sim 200\mu$ G). The resulting unpulsed emission from radio to gamma rays up to 100 MeV is interpreted as synchrotron radiation from at least two populations of electrons/positrons energized by the pulsar wind and by surrounding shocks or plasma instabilities (e.g., Atoyan & Aharonian [1996], Meyer et al. [2010]). The optical and X-ray brightness enhancements observed in the inner Nebula, known as “wisps”, “knots”, and the “anvil” aligned with the pulsar “jet” (Scargle [1969]; Hester [1995], [2008]; Weisskopf [2000]), show flux variations on timescales of weeks or months. On the other hand, the average unpulsed emission from the Crab Nebula was always considered essentially stable. The surprising discovery by the AGILE satellite of variable gamma-ray emission from the Crab Nebula in Sept. 2010 [Tavani et al. 2010, 2011a], and the Fermi-LAT confirmation [Abdo et al. 2011, Buehler et al. 2010] started a new era of investigation of the Crab system. As of Sept. 2012 we know of four major gamma-ray flares from the Crab Nebula detected by the AGILE Gamma-Ray Imaging Detector (GRID) and Fermi-LAT: (1) the Sept-Oct. 2007 event, (2) the Feb. 2009 event, (3) the Sept. 2010, and (4) the “super-flare” event of Apr. 2011 (Buehler et al. [2011]; Tavani et al. [2011b]; Hays et al. [2011]; Striani et al. [2011a]; Striani et al. [2011b]; Buehler et al. [2012]).

In this proceeding we address the issue of the gamma-ray variability of the Crab Nebula on different timescales ranging from days to weeks. We then enlarge the parameter space sampled by previous investigations especially for the search of statistically significant enhanced emission on timescales of 1-2 weeks. We will present a brief overview of the current knowledge on Crab’s main gamma-ray flares and the results of a search of γ -ray enhanced emission on timescales of weeks in the AGILE and Fermi-LAT database and a brief discussion of our results. This proceeding is based on Striani et al. [2013], where the data analysis and discussion are presented with more details.

2. Overview of the main gamma-ray flares

Four major episodes of intense gamma-ray flaring from the Crab Nebula have been detected by AGILE and Fermi-LAT [Abdo et al. 2011, Buehler et al. 2012, Striani et al. 2011b, Tavani et al. 2011a, Vittorini et al. 2011]. The definition of a “flare” adopted in this paper is that of a single gamma-ray enhancement event with a risetime $\tau_1 < 1$ day and flux $F > 700 \times 10^{-8}$ ph cm⁻² s⁻¹ above 100 MeV. Table 1 summarizes the flaring events that we find by considering the AGILE and the publicly available Fermi-LAT database. These events show a complex time structure, being composed of several sub-flares that we classify as Fn' , with n' a progressive number. Fig. 1 summarizes the four major flaring episodes with the same temporal and flux scales. The colored curves are indicative of the flaring behavior that in most cases can be represented by an exponential fit, characterized by rising (τ_1) and decay (τ_2) timescales as given in Table 1. We also report in Table 1 the

Table I Table of the *flares* ($F \geq 700 \times 10^{-8} \text{ ph cm}^{-2} \text{ s}^{-1}$) of the Crab Nebula found in the AGILE and Fermi data from Sept. 2007.

	Name	MJD	τ_1 (hr)	τ_2 (hr)	Peak Flux	B (mG)	γ^* (10^9)	l (10^{15} cm)
2007 (AGILE)	F_1	54381.5	22 ± 11	10 ± 5	1000 ± 150	1.0 – 2.0	2.6 – 4.8	1.2 – 3.6
	F_2	54382.5	14 ± 7	6 ± 3	1400 ± 200	1.1 – 2.1	2.3 – 4.3	0.8 – 2.2
	F_3	54383.7	11 ± 5	14 ± 7	900 ± 150	1.0 – 2.0	2.6 – 4.8	0.8 – 1.7
2009 (FERMI)	F_4	54865.8	10 ± 5	20 ± 10	700 ± 140	0.7 – 1.3	2.6 – 4.8	0.6 – 1.6
	F_5	54869.2	10 ± 5	22 ± 11	830 ± 90	0.8 – 1.4	2.6 – 4.8	0.6 – 1.6
2010 (AGILE & FERMI)	F_6	55457.8	8 ± 4	22 ± 11	850 ± 130	0.7 – 1.3	2.5 – 4.7	0.5 – 1.3
	F_7	55459.8	6 ± 3	6 ± 3	1000 ± 100	1.4 – 2.6	2.6 – 4.8	0.3 – 0.9
	F_8	55461.9	19 ± 10	8 ± 4	750 ± 110	0.8 – 1.4	2.5 – 4.8	0.9 – 3.1
2011 (FERMI & AGILE)	F_9	55665.0	9 ± 5	9 ± 5	1480 ± 80	1.2 – 2.2	2.8 – 5.0	0.5 – 1.5
	F_{10}	55667.3	10 ± 5	24 ± 12	2200 ± 85	1.3 – 2.3	2.7 – 4.9	0.6 – 1.6

The timescales τ_1 and τ_2 are the rise and decay timescales of the flares modelled with an exponential fit respectively.

The characteristic length of the emitting region is deduced from the relation $l = c \delta \tau_1$. The Lorentz factor γ^* characterizes the adopted model of the accelerated particle distribution function $dn/d\gamma = K/\alpha \cdot \delta(\gamma - \gamma^*)$, where K is defined in the spherical approximation. $\alpha = 1$ in the spherical case, and $\alpha < 1$ for cylindrical or pancake-like volumes reproducing the current sheet geometry. The peak photon flux above 100 MeV is measured in units of $10^{-8} \text{ ph cm}^{-2} \text{ s}^{-1}$.

These parameters are obtained, by means of a multi-parameter fit, from the following quantities (in the observer frame): the position of the peak photon energy, $E_p \propto \delta \gamma^{*2} B$, the peak emitted power $\nu F \propto \delta^4 K/\alpha l^3 B^2 \gamma^{*2}$, the rise time $\tau_1 = l/(c\delta)$, and the cooling time $\tau_2 = 8.9 \times 10^3 / [(B/\text{Gauss})^2 \gamma^{*2} \delta]$, assuming $\delta = 1$ (see text).

data fitting physical parameters (average local magnetic field B , typical particle Lorentz factor γ^* , and characteristic size l of the emitting region of the flaring episodes). We determine these parameters and their uncertainties from the time constants τ_1 and τ_2 . Whenever applicable (2010 and 2011 events), the AGILE and Fermi-LAT data are consistent both in flux and spectral properties.

3. The September-October 2007 event detected by AGILE

Fig. 2 shows the 1-day lightcurve ($E > 100 \text{ MeV}$) of the Crab (pulsar plus Nebula) between Sept. 24, 2007 and Oct. 13, 2007. with a zoom of the lightcurve focused on the short variability episodes in the inset. The χ^2 analysis of this data show that there are 2 regions of enhanced emission that are more than 5 sigma (in a 7-day timescale) above the Crab average flux in the AGILE data. These regions have an average flux of $\sim 450 \times 10^{-8} \text{ ph cm}^{-2} \text{ s}^{-1}$ and a rise and decay time of the order of several days. These slow components of enhanced γ -ray emission show features different than those of flares that typically have rise and decay times of the order of 12-24 hr, and peak fluxes ranging from $F_{p,5} \simeq 800 \times 10^{-8} \text{ ph cm}^{-2} \text{ s}^{-1}$ up to $F_{p,10} \simeq 2500 \times 10^{-8} \text{ ph cm}^{-2} \text{ s}^{-1}$ (as for the Crab super-flare of Apr. 2011). We call these slow component of enhanced emission *waves*. We indicate with W_1 the emission from MJD $\simeq 54367$ to MJD \simeq

54374 and with W_2 the emission from MJD $\simeq 54376$ to MJD $\simeq 54382$. The 12-hr lightcurve in the inset of Fig. 2 shows that the 2007 peak intensity event, that in our previous analysis [Tavani et al. 2011a] appeared unresolved, is actually composed of three different flaring components, that we indicate by F_1 , F_2 , and F_3 . Peak fluxes, rise times and decay times (estimated with an exponential fit) for F_1 , F_2 , and F_3 and for W_1 and W_2 are presented in Tab. I. The post-trial probability, $P_{post} = 1 - (1 - p)^{N_t}$, with p the pre-trial probability obtained from the χ^2 test, and N_t the number of 7-day maps (trials), is $P_{post} > 5\sigma$ for both W_1 and W_2 . We find that the differential particle energy distribution function (per unit volume) can be described by a monoenergetic function, $dn/d\gamma = K/\alpha \cdot \delta(\gamma - \gamma^*)$, where γ is the particle Lorentz factor, and γ^* is the monochromatic value of the particle energy. The electron density constant K is defined in the spherical approximation, with $\alpha = 1$ in the spherical case, and $\alpha < 1$ for cylindrical or pancake-like volumes. A power-law distribution and/or a relativistic Maxwellian distribution were also shown to be consistent with the flaring data (Tavani et al., [2011a], Striani et al. [2011b]). We adopt here a monochromatic distribution that deconvolved with the synchrotron emissivity leads to an emitted spectrum practically indistinguishable from the relativistic Maxwellian shape (e.g., Striani et al. [2011b], Buehler et al. [2012]). This distribution is in agreement with all available gamma-ray data (for both flaring and “wave” behavior, see below), and reflects an

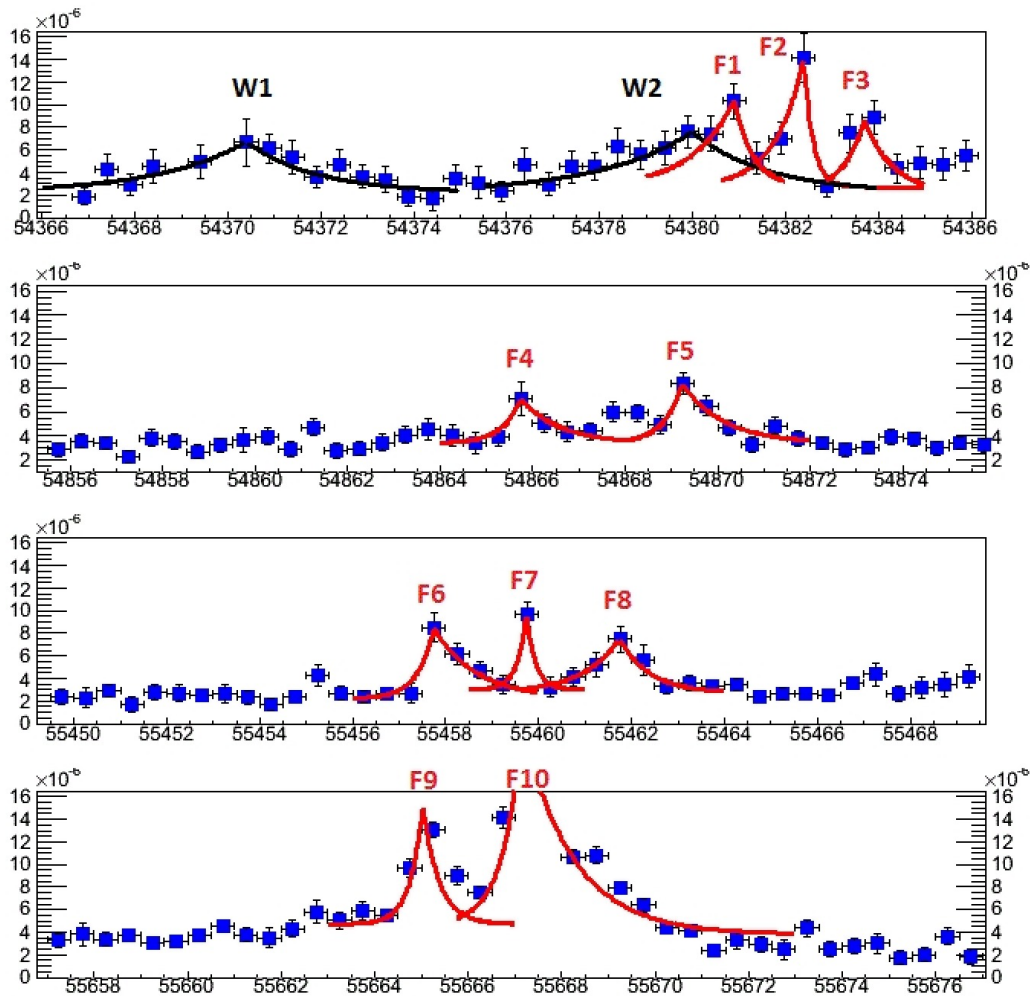


Figure 1: Gamma-ray lightcurves above 100 MeV (12-hr time bins) from the Crab (pulsar plus Nebula) detected by AGILE and Fermi-LAT. From top to bottom, the Sept. - Oct. 2007 event (AGILE data), the Feb. 2009 event (Fermi-LAT data), the Sept. 2010 event (Fermi-LAT data), and the Apr. 2011 event (Fermi-LAT data).

important property of the flaring Crab acceleration process (Tavani [2013]). With our calculations we find for W_1 a magnetic field $B = (0.8 \pm 0.2)$ mG, a Lorentz factor $\gamma^* = (4 \pm 1) \times 10^9$, and a typical emitting length range $l = (0.5 - 1.5) \times 10^{16}$ cm. For F_2 , we find $B = (1.5 \pm 0.5)$ mG, $\gamma^* = (3 \pm 1) \times 10^9$, and $l = (1.5 \pm 0.7) \times 10^{15}$ cm. In our model, the total number of accelerated particles producing the gamma-ray wave/flaring behavior is in the range $N \sim (1 - 3) \cdot 10^{38} (\Delta\Omega/4\pi)$, with $\Delta\Omega$ the solid angle of the γ -ray emission. It is interesting to note that besides the differing values of the magnetic field and particle densities, the typical Lorentz factor and total number of radiating particles are similar for the “wave” W_1 and the flare F_2 . We find that this is a typical behavior of the transient gamma-ray emission that appears to be well represented by a monochromatic particle distribution function with $\gamma^* \simeq (3 - 5) \times 10^9$.

4. Search for enhanced gamma-ray emission in the Fermi-LAT data

Motivated by the waves found in the AGILE data, we searched for a similar type of enhanced gamma-ray emission in the publicly available Fermi-LAT data. With our χ^2 analysis of the Fermi data we identified four episodes of enhanced gamma-ray emission that are, in a 8-days timescale, more than 5-sigma above the Crab average flux. We call them W_3, W_4, W_6 and W_7 in Fig. 3. These episodes have apparent durations in the range from 8 to 50 days (see the complex marked as $W_3 - W_4$), and an average flux in the range $F = (350 - 500) \times 10^{-8}$ ph cm $^{-2}$ s $^{-1}$. The event W_7 is

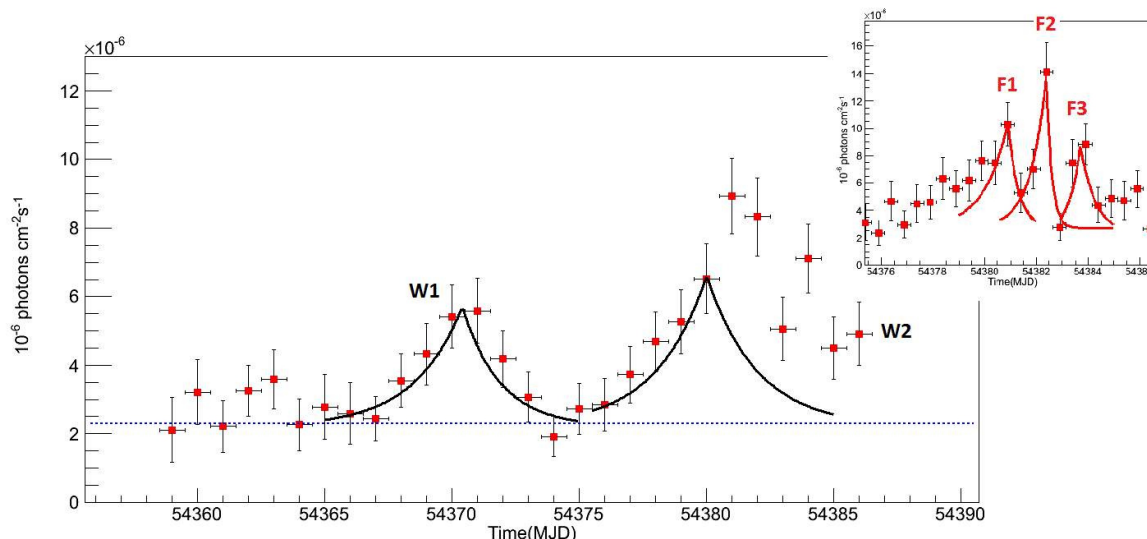


Figure 2: Lightcurve (1-day bin) of the Sept.- Oct. 2007 Crab Nebula flare detected by AGILE. In the inset the 12-hr bin lightcurve around the flare. This episode is characterized by a very strong variability, with waves (black line, marked with a W) and flares (red line, marked with an F .)

coincident with the enhancement episode detected¹ by Fermi-LAT (Ojha et al., 2012). Fig. 3 shows the detailed lightcurves of the Fermi-LAT wave episodes with the largest post-trial significance. Fig. 3 shows a remarkable episode of “wave” enhanced emission near MJD = 55000. The Crab was for about 50 days above 5σ from its standard gamma-ray flux, with an average flux in this period $F = (340 \pm 6) \times 10^{-8} \text{ ph cm}^{-2} \text{ s}^{-1}$. This event appears quite complex². The total episode that includes f^* , W_3 and W_4 has a time duration of ~ 50 days, a pre-trial probability $p = 2 \times 10^{-25}$ and a post-trial significance $\sigma_{post} > 10$. For each “wave” that we found at 5σ above the Crab average emission, we estimated the rise τ_1 and the decay time τ_2 , the average flux, the peak flux, the probability of obtaining the given χ^2 in the null hypothesis, and the post-trial significance. The rise and decay timescales are estimated with an exponential fit. The results are summarized in Tab. 2.

5. Constraints from a synchrotron cooling model

We can deduce important physical parameters of the enhanced γ -ray emission by adopting a syn-

¹Due to solar panel constraints, this event was unobservable by AGILE.

²For simplicity, we use an exponential approximation for the “wave” emission. Admittedly, this approximation for the episode of Fig. 3 centered on MJD = 55000 is not adequate. It is shown in Fig. 3 for illustrative purposes only.

chrotron cooling model (see also Tavani et al. [2011a], Vittorini et al. [2011], Striani et al. [2011b]). Tables 1 and 2 summarize the relevant information for the major “flares” and “waves”. We find that for flares lasting 1-2 days the typical length is $l \simeq (1 - 2) \times 10^{15}$ cm, the density constant in the range $K/\alpha = (2 - 8) \times 10^{-9} \text{ cm}^{-3}$, the typical Lorentz factor $\gamma^* = (2.5 - 4.5) \cdot 10^9$, and the local magnetic field affecting the cooling phase in the range $B = (1 - 2)$ mG. As discussed above, the total number of radiating particles, in case of unbeamed ($\delta = 1$) isotropic emission, is $N \sim (1 - 3) \cdot 10^{38}$.

For the “wave” episodes, the typical length is $l > 10^{16}$ cm, the density constant is in the range $K/\alpha = (2 - 8) \times 10^{-11} \text{ cm}^{-3}$, the Lorentz factor $\gamma^* = (3 - 5) \cdot 10^9$, and the local magnetic field in the range $B = (0.5 - 1)$ mG. The total number of particles involved is of the same order as in the case of flares.

6. Discussion and Conclusions

By considering AGILE and Fermi-LAT gamma-ray data above 100 MeV we find that the Crab produces a broad variety of enhanced emission. We characterize this enhanced emission as short timescale (1-2 day) “flares” and long timescale (1 week or more) “waves”. Given the current detection level of 1-2 day enhancements (which can be extended to longer timescales of order of 1-2 weeks), we cannot exclude that the Crab is producing an even broader variety (in flux and timescales) of enhanced gamma-ray emission. With the current sensitivities of γ -ray telescopes we can explore an important but necessarily limited range of

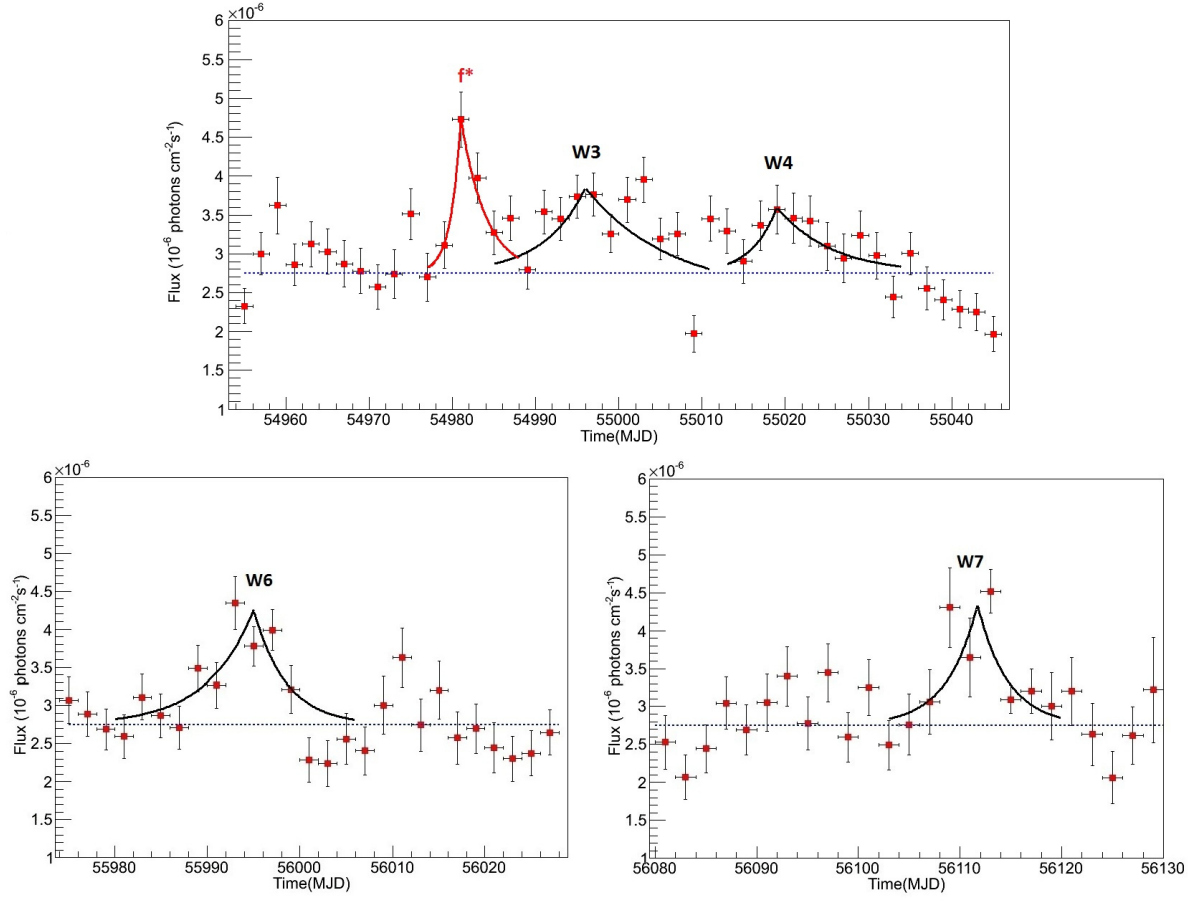


Figure 3: The most prominent *wave* episodes in the Fermi-LAT data with more than 5σ enhancements above the Crab average emission. 2-day binned gamma-ray flux values (in unit of 10^{-6} ph cm^{-2} s^{-1}) above 100 MeV as a function of time. We notice that the event marked as f^* is intermediate between flares and waves.

Table II Table of the *waves* above 5σ post-trial from the Crab average emission found in the AGILE and Fermi data.

Name	MJD	Duration (days)	τ_1 (days)	τ_2 (days)	Average Flux (10^{-8} ph cm^{-2} s^{-1})	Peak Flux (10^{-8} ph cm^{-2} s^{-1})	Pre-trial p-value	Post-trial significance
W_1	54368-54373	5	2 ± 1	2 ± 1	440 ± 40	670 ± 200	4.5×10^{-8}	5.0
W_2	54376.5-54382.5	6	2.5 ± 1	2 ± 1	480 ± 40	760 ± 140	3.0×10^{-9}	5.5
W_3	54990-55008	18	5 ± 2.5	10 ± 5	352 ± 9	380 ± 30	1.0×10^{-8}	4.6
W_6	55988-56000	12	5 ± 2.5	3.5 ± 1.5	367 ± 12	435 ± 35	1.8×10^{-12}	6.2
W_7	56108-56114	6	3 ± 1.5	3 ± 1.5	431 ± 22	450 ± 30	1.9×10^{-9}	5.9

Photon fluxes are obtained for $E_\gamma > 100$ MeV.

flux and spectral variations. It is interesting to note that what we called “flares” and “waves” (a somewhat arbitrary division) share the same spectral properties. Given the current gamma-ray sensitivities, we could have detected different spectral behaviors in the energy range 50 MeV - 10 GeV. Most likely, flares and waves are the product of the same class of plasma instabilities that we show acting on different timescales and radiation intensities. Whether or not the insta-

bility driver of this process is truly stochastic in flux and timescales will be determined by a longer monitoring of the Crab Nebula. The pulsar wind outflow and nebular interaction conditions need to be strongly modified by instabilities in the relativistic flow and/or in the radiative properties. Plasma instabilities possibly related to magnetic field reconnection in specific sites in the Nebula can be envisioned. However, evidence for magnetic field reconnection events in the

Crab Nebula is elusive, and no optical or X-ray emission in coincidence with the gamma-ray flaring has been unambiguously detected to date (e.g., Weisskopf et al. [2012]).

Both the flaring and “wave” events can be attributed to a population of accelerated electrons consistent with a mono-chromatic or relativistic Maxwellian distribution of typical energy $\gamma^* \sim (2.5 - 5) \cdot 10^9$.

We also notice that the emitted total energies that can be deduced for the wave ($\delta E_{\gamma,w}$) and flare ($\delta E_{\gamma,f}$) episodes in general satisfy the relation $\delta E_{\gamma,w} \simeq \delta E_{\gamma,f}$. The total gamma-ray emitted energy for the wave episode W_1 can be estimated as $\delta E_{\gamma,w1} \sim 10^{41}$ erg. Therefore, the energy associated with the wave event W_1 , taken here as an example of Crab “wave” emission, can reach a few percent of the total spindown energy.

We conclude that the Crab “wave” events are highly significant and quite important from the energetic point of view. “Waves” typically imply regions larger than in the case of flares, and smaller average magnetic fields. Their total emitted gamma-ray energy can be comparable with that associated with shorter flares. More observations of this fascinating phenomenon are necessary to improve our knowledge of the flaring Crab.

References

Abdo, A.A., et al., 2011, *Science*, **331**, 739.

- Atoyan, A.M. & Aharonian, F.A., 1996, *MNRAS*, **278**, 525.
- Buehler, R., *et al.*, 2010, *Astron. Telegram* 2861.
- Buehler, R., *et al.*, 2011, *Astron. Telegram* 3276.
- Buehler, R., Scargle, J. D., Blandford, R. D., et al. 2012, *ApJ*, **749**, 26
- Hays, E., *et al.*, 2011, *Astron. Telegram* 3284.
- Hester, J.J., P. A. Scowen & R. Sankrit *et al.*, 1995, *ApJ*, **448**, 240.
- Hester, J.J., Mori, K., Burrows, D. *et al.*, 2002, *ApJ*, **577**, L49.
- Hester, J.J., 2008, *Annual Rev. Astron. & Astrophys.*, **46**, 127.
- Meyer, M., Horns, D. & Zechlin, H.S., 2010, *A&A*, **523**, A2.
- Ojha, R., et al., 2012, *Astron. Telegram* 4239.
- Pittori, C., Verrecchia, F., Chen, A. W., et al. 2009, *A&A*, **506**, 1563
- Scargle, J.D., 1969, *ApJ*, **156**, 401.
- Striani, E., Tavani, M., Vittorini, V., et al. 2013, *ApJ*, **765**, 52
- Striani, E., *et al.*, 2011a, *Astron. Telegram* 3286.
- Striani, E., Tavani, M., Piano, G., et al. 2011b, *ApJL*, **741**, L5
- Tavani, M. *et al.*, 2010, *Astron. Telegram* 2855.
- Tavani, M., *et al.*, 2011a, *Science*, **331**, 73.
- Tavani, M., *et al.*, 2011b, *Astron. Telegram* 3282.
- Tavani, M., 2013, in preparation.
- Vittorini, V., *et al.*, 2011, *ApJ*, **732**, L22.
- Weisskopf, M.C., Hester, J.J., A. F. Tennant, R. F. Elsner, N. S. Schulz *et al.*, 2000, *ApJ*, **536**, L81.
- Weisskopf, M. C., Tennant, A. F., Arons, J., et al. 2013, *ApJ*, **765**, 56